Resistive switching in Al/Tb/SiO_2 nano-multilayers

Albert Doblas Moreno
Blas Garrido Fernández and Oriol Blázquez Gómez
MIND-IN^{2}UB, Departament d'Electrònica, Universitat de Barcelona, Martí i Franqués 1, 08028, Barcelona, Catalonia, Spain

***Abstract*—Resistive switching mechanism in memristors offers wide novel properties for nanoelectronics devices. In this work, we report an Al/Tb/SiO_2 nano-multilayer memristor. Our devices were fabricated in terms of electron beam evaporation with thicknesses in the order of nanometres. Our devices exhibit memristive behaviour with a high change in resistance which can be cycled up to 20 times at room temperature. The states can persist at least for 140 h. We report bipolar switching with set and reset voltages with a low dispersion during the cycling. We have also studied the impact of the compliance current. Additionally, we studied which conduction mechanism is carrying out the memristive behaviour of our samples, where an Ohmic conduction in the low resistance state is observed and a Schottky fit is applied at the high resistance state. Current-time characteristics of the devices is also shown, where fluctuations and the time of commutation are presented. Finally, we also report the structural characterization of another type of samples, where only the switching mechanism is the aim of study. We have supposed that valence change mechanism is the responsible for the switching mechanism.**

***Index Terms*—4. Nanoelectronics: memristor, resistive switching, non-volatile memories, nano-multilayers, electron beam evaporation.**

I. Introduction

MEMRISTORS are two terminal devices based on the resistive switching (RS) mechanism. The concept of memristor was postulated for the first time by Leon Chua at 1971 as the *missing* fourth passive circuit element [1], but since 2008 the first practical realization (titanium oxide) was not reported [2]. We talk about RS phenomenon when a device presents two conductive states: a high resistance state (HRS) or a low resistance state (LRS). A conductive path that is connected and disconnected is created, allowing the device to commute between both states. Therefore, applying a certain voltage one can pass from the HRS to LRS (V_{set}) and from LRS to HRS (V_{reset}). First voltage applied to pass from HRS to LRS is called the forming or electroforming voltage ($V_{forming}$), which is typically lower than V_{set}. In all the processes where the device commutes from a state to another, the current is limited by the system with the current compliance (I_C) to avoid that the current in LRS shoots up. In each memristor device, the commutation phenomenon is observed in a different way and, therefore, it is necessary to make a distinction in function of the polarity of the set and reset processes.

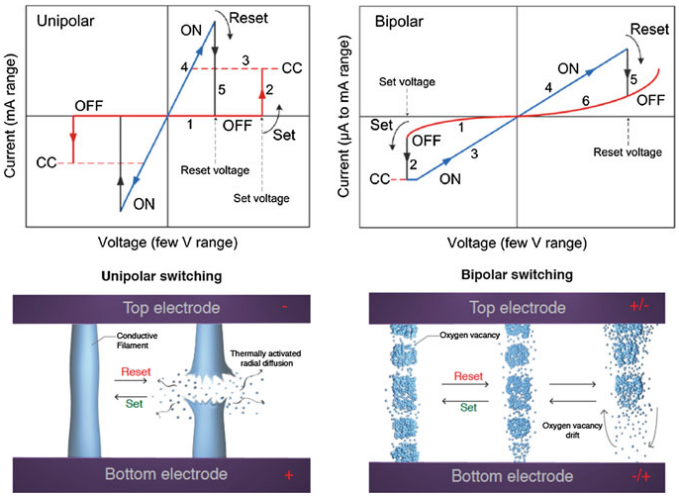

***Fig. 1.** Typical hysteretic curve for the resistive switching mechanism. **Left**: unipolar switching mode, where the set and reset processes are in the same range of voltage (positive or negative) and a sketch of how set and reset processes affect to the conduction filament. **Right:** bipolar switching mode, where the set and reset processes occurs in different voltage polarities. Sketch of the movement of oxygen vacancies during reset and set processes in a bipolar switching. Extracted from [3].*

In a unipolar switching, the commutation phenomenon depends on the voltage applied but not in its polarity. On the other hand, in a bipolar switching, the set process occurs in a different polarity that reset process. RS mechanism can be also classified as a function of the physical mechanism that allows the commutation between two states. A wide of physical mechanisms are known. One of the most employed are electrostatic and electronic effects, like change from crystalline phase (ON) to amorphous phase (OFF), induced by temperature (in tellurides and selenides). Besides, there are three classes which involve chemical effects, that is, effects which relate to redox process in the device induced by either temperature or electrical voltage or both: electrochemical mechanism (ECM), thermochemical mechanism (TCM) and valence change mechanism (VCM). ECM cells behave always with bipolar switching. A conduction filament (CF) is formed from an active metallic electrode to an inert electrochemical anode through an ion conductive insulating layer. By applying a voltage at the cathode, a conduction of ions appears at the insulating layer through the cathode and the CF begins to forming since it reaches the cathode (set). By applying a

negative voltage, the reset process appears and also the rupture of the CF. On the other hand, TCM mechanism is based in a thermal effect which is always presented as unipolar switching. This effect is produced due to structural changes as a consequence of an increase in temperature. A small path can be created by Joule effect with a controlled resistivity. Finally, VCM process occurs in metallic oxides. In this case, the RS mechanism is produced by a migration of oxygen anions (known as *oxygen vacancies*). There is a change in the valence of ions which changes the conductive properties of the material. There are two models where VCM is defined: commutation along a filament that not depends on the area and commutation distributed at the interface metal-dielectric, which depends on the area.

Typically, the study of RS is done in MIM (metal-insulator-metal) structures. However, the study in MOS (metal-oxide-semiconductor) structures can be interesting due to non-lineal conduction characteristics. Due to the fact that silicon is present in a high percentage of CMOS technology, SiO_x memristors have huge interest in research [4]. First silicon oxide study reported a switchable silicon conductive path formed on the vertical surface of a silicon-rich silica pillar [5]. Most promising metal oxides used in RS devices are NiO [6], TiO_x [7], HfO_2 [8] and the aforementioned SiO_x, among others.

Non-volatile resistive random access memories (RRAM) are the main application of memristor devices. Using the huge difference in resistance of the two states, each of them can be defined as a "1" or a "0", as a classical bit. In order to obtain a good non-volatile memory, the change in resistance between two states has to be at least two order of magnitude. Another application of RS phenomenon is the implementation of artificial neural networks. Thanks to the excellent memristor features like large scalability, very low power consumption, great endurance, fast switching speed and the multilevel switching behaviour, the scientific community has a huge interest in the use of memristive device as synapses. In [9], they can be able to model the electrical activity of a neuron using a RRAM cell. Stochastic computing and security can be also some new applications of the memristors using their huge spatial variability and the fact that memristive devices present stochastic nature in their parameters [10].

In this work we report an Al-Tb/SiO_2 nano-multilayer (NML) memristor device that can be cycled several times under ambient conditions with a high change in resistance from the HRS to the LRS. Both states are stable, persisting for at least 140h.

II. Experimental Details

A. Fabrication and devices

Our memristor device consists of Al-Tb/SiO_2 nano-multilayer (NML) structure [Fig. 2] which were fabricated by means of electron beam evaporation (EBE) technique onto crystalline (100)-Si substrate, using a PFEIFFER VACUUM Classic 500 instrument with a Ferrotec GENIUS electron beam controller and a Ferrotec CARRERA high-voltage power supply. Before deposition, substrates were cleaned with acetone, isopropyl alcohol, ethanol, and de-ionized water, and agitated ultrasonically during each process. Nanometric layers of SiO_2, Al and Tb were alternatively deposited. In this work, the NML structure consists of a stack of 5x Al/Tb/Al/SiO_2 layers with a nominal thickness of 0.8, 0.4, 0.8 and 3 nm, respectively. In order to protect the Al/Tb/Al/SiO_2 stack from the following annealing treatment, two 10 nm SiO_2 layers were deposited at the bottom and top of the structure. The Al electrodes were deposited using a mask where the Al dots had a radius of 100, 150 and 200 µm. The base pressure in the chamber was 1.8 x 10^{-6} mbar and the temperature of the substrate was kept to 100 ºC. The nominal deposition rates were 0.2, 0.2 and 1.0 Å/s for Al, Tb and SiO_2, respectively, and using an electron beam acceleration voltage of either 10 kV for Al and 6 kV for Tb and SiO_2. After the deposition process, the sample was annealed at a T=1100 ºC.

In order to study morphologically our devices, we made a different type of samples. In this case, the structure of the devices was exactly the same than the sketch of figure 2 with the difference that the Al/Tb/Al stack is removed and the samples are as-deposited (without annealing treatment).

B. Experimental measurements

Electrical characterization of the devices was performed with the commercial system Agilent B1500a semiconductor device analyser using different experimental approaches. Current that pass through our devices has the order of pico- and nano-amperes. Therefore, we need an experimental system capable to detect such small currents. We employed a system with four very small and sharp probes (Microtech Summit 11000) that touch the top electrodes of our samples. The bottom electrode is connected to the chuck of the system which acts as a ground to close the circuit. In order to study the memristive behaviour, we had to observe the I-V curve, where a certain voltage has been ramped up (with a 50 mV step) until a convenient value and then it was brought to zero.

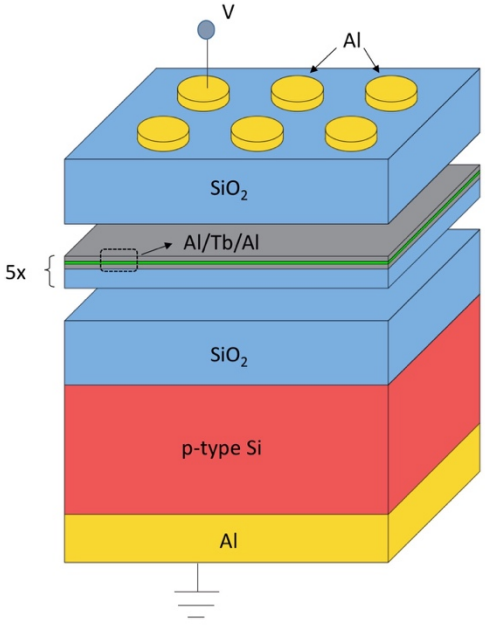

Fig. 2. *Sketch of the NML device where the structure and type of materials are shown.*

This process has been carried out for positive and negative voltages. The aforementioned compliance current is a parameter that has been changed depending on the type of measurement desired. For the positive range, the compliance current is set in different values, but, on the contrary, for negative values of voltage we set the compliance current to the maximum value (50 mA). In order to study if the device can be cycled several times, the previous experimental procedure is repeated for each cycle. We talk about a cycle when the device passes from the HRS to LRS and then return from LRS to HRS. With this equipment, a study of how current varies in a range of time can also be done. We had to define a certain value of voltage, a range of time and a time step. In all the measurements we employed a time step of 500 ms and 60 s of measurement. We focused on the electrical characterization of these devices.

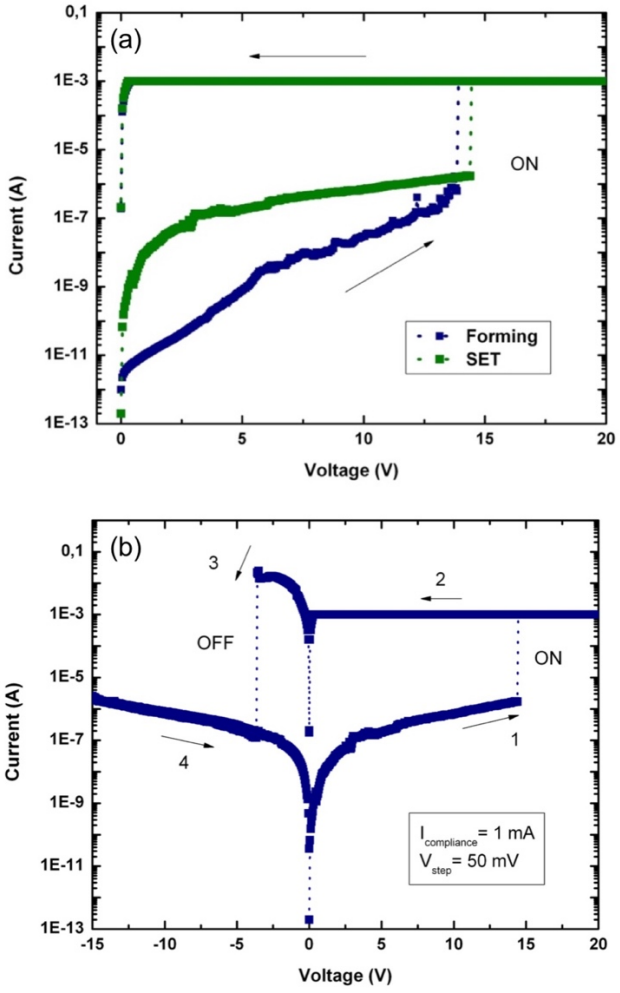

***Fig. 3**. Current-voltage characteristics of a memristor device with a I_C =1 mA and V_{STEP}=50mV. Arrows indicate the direction of voltage cycling. **(a)** Comparison between the forming process (first set) and set process in (b). It is shown the difference in set voltage and also in the current passing through the device. **(b)** Full cycle where the system is in the HRS (OFF) until it reaches the set process (1) where it jumps to the LRS (ON) and remains in this state due to compliance current (2). In the reset process (3) the device passes from the ON state to the OFF state until voltage return to 0 V (4).*

Second type of samples are used to study a morphological characterization. To perform the structural characterization, we employed Scanning Electron Microscopy (SEM) to obtain an image of the devices before and after the set process and Energy-Dispersive Spectroscopy (EDS) to perform an elemental characterization of the devices (Jeol JSM-7100F). These second type of samples were not electrically characterized due to they are not optimal to perform resistive switching mechanism.

III. RESULTS AND DISCUSSION

A. Current-voltage characteristics

The pristine state of the devices is generally high resistance. The current passing through the device is in the order of pico- and nano-amperes. However, applying a voltage stress at the device, we can pass to a state with low resistance. The forming process usually has a lower voltage to commute from OFF to ON than the set process. Fig. 3(a) shows the first cycle (forming) and the set process for another cycle. We can extract from this graph the difference in current from the two process. In the forming process, the current passing through the device is lower than the set process, which demonstrates the fact that in the forming process the filaments are being created. The current is huge in the set process due to the filaments are already created. In our case, the difference in voltage from pass to the ON state is very low. Fig. 3(b) shows typical I-V results. The device is in the HRS (OFF) state until it reaches V_{set} and jumps to the LRS (ON). Later on, the system remains in the ON state when the system is decreasing the voltage, that is limited by I_C. For negative values, the device is in the ON state until it reaches V_{reset} and falls down to the OFF state again. In this certain cycle, we achieve values of V_{set} = 14.5 V and V_{reset} = -3.6 V. We can also extract the values of the resistance in both states. For the ON state we obtain a value of 165 Ω and for the OFF state a value of 30 MΩ. A huge difference in resistance is obtained for this cycle. It is clear that this behaviour corresponds to a bipolar resistive switching mechanism, owing to different polarities for the set and reset processes.

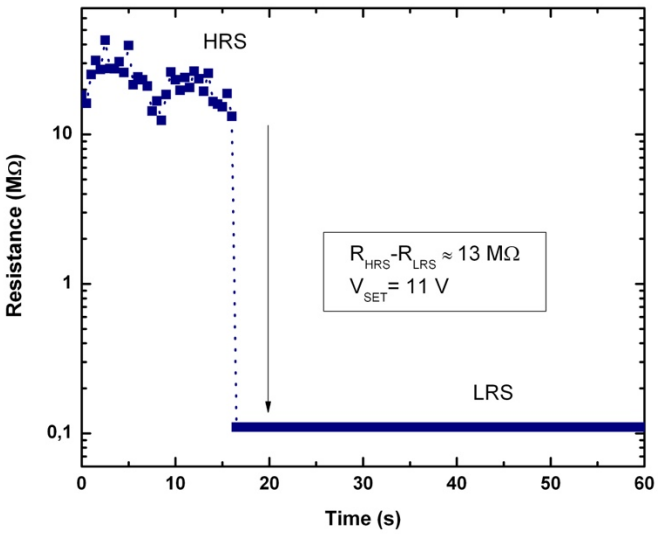

***Fig. 4.** Resistance as a function of the time for a V_{set} =11 V device. There is a change of 13 MΩ between both states.*

The device is not able to perform a whole cycle without changing the voltage polarity, therefore this device is not showing a unipolar switching mechanism. A fall in resistance is observed due to increase in current when the system passes from the HRS to the LRS [Fig. 4]. The HRS presents a resistance of 13.2 MΩ, while for the LRS the resistance we extracted a value of 0.1 V. It is also seen the fluctuations in resistance (or current) in a certain period of time. However, at the LRS there is no fluctuations due to the compliance current.

A. Cycling and memristor parameters

Our device has been able to hold at least 20 cycles. Fig. 5(a) shows the I-V curve for the 20 cycles. It can be seen a difference in the I-V characteristics of the first three cycles and the rest. First cycle is the forming process and second and third have the same behaviour. From fourth cycle, the I-V curve stabilizes, which means that the forming process is over. We can interpret this assuming that the forming process has not been carried out since the fourth cycle.

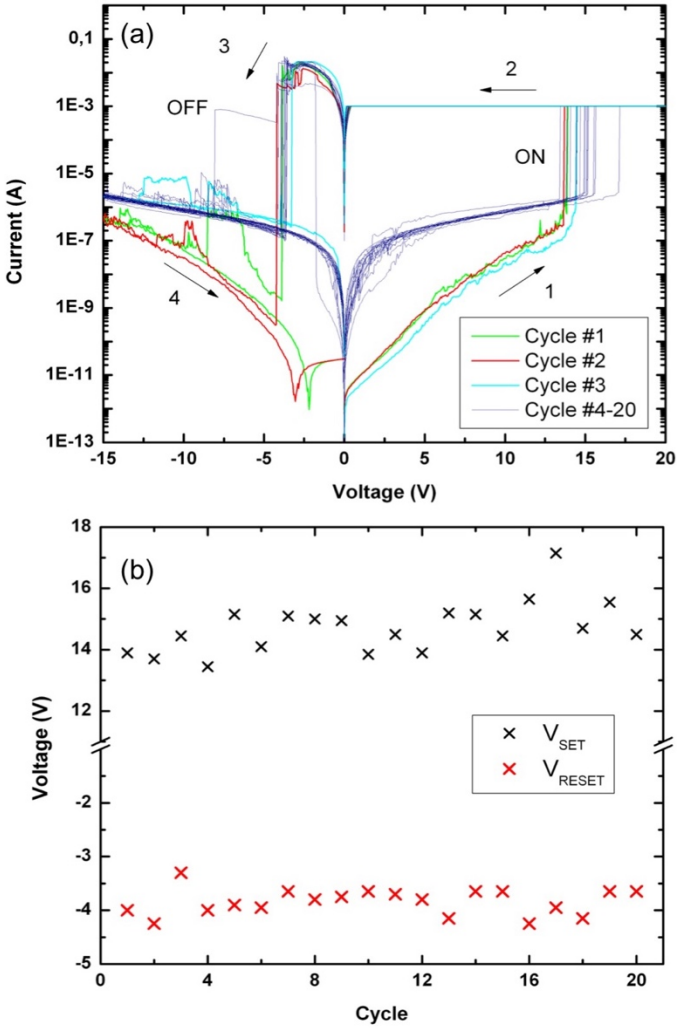

Fig. 5. (a) *Cycling of the device. There are differentiated the first three cycles from the rest, in order to see the different behaviour. Our device has been able to hold at least 20 cycles with a set and reset voltage dispersion.* ***(b)*** *Voltage set (black) and reset (red) as a function of the cycle. For the reset voltage the dispersion is lower than the set process.*

This can be due to charge carrier concentration. From this graph we can also extract information about the set and reset voltages. In each cycle, the voltages change and there is a dispersion of its value. This dispersion is shown in Fig. 5(b). A values of V_{set} = 14.7 ± 0.8 V and V_{reset} = -3.6 ± 0.3 V are extracted. Therefore, the reset process has a lower dispersion than the set process. Anyway, both voltage values have a low error and the dispersion error is not too high. In addition, if we want to prepare a portable non-volatile memory, the values of set and reset have to be a few volts. Therefore, the set voltage would be decreased. Assuming that we need low voltages to perform the set and the forming process, we could build another device with lower thicknesses in order to help the nanofilament to arrive from bottom electrode to top electrode easily. Another solution would be use another element instead of terbium.

Another interesting parameter to consider is the compliance current. Our devices need this value to avoid damages and to control the memristive cycle. Our experimental system allows us to work in the range [1μA-50mA]. We have studied the different extremes of the I_C. For negative voltages our compliance current was always 50 mA and the only value that we changed is the I_C for positive voltages, because the reset process always needs a huge current to reach the HRS. Cycles from Fig. 5(a) are done with a current compliance of 1 mA, that is a high value. Optimum value of compliance current is 1 μA, since it is the lowest value achievable. We have been able to perform a cycle using this value [Fig. 6]. However, we have observed that our device could perform a cycle with a lower value, but our system did not permit it. On the contrary, for a value of 50 mA, our device has not been able to pass from the LRS to the HRS due to the high current passing through it. The maximum value obtained that allows us to observe a whole cycle was 10 mA. From this value was very difficult to perform the reset process. In conclusion, the work range of our device is [1-10^4] μA. However, this device works much better from hundreds of μA to a few of mA. Figure 6 shows the two I-V curves for each current compliance.

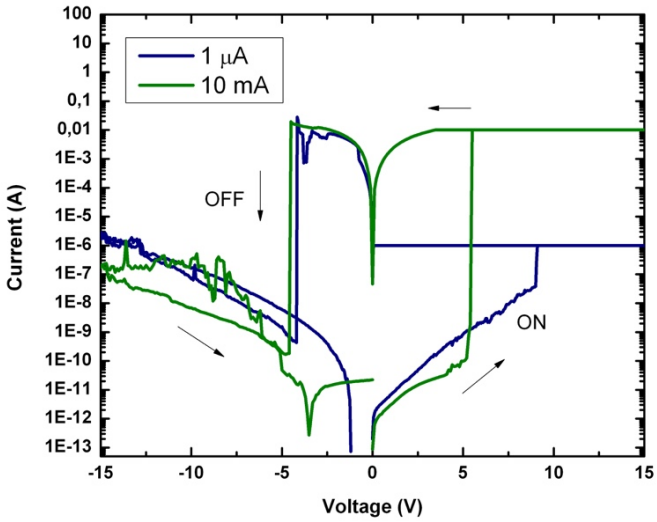

Fig. 6. *I-V characteristics for the highest (green) and the lowest (blue) compliance currents. The set voltage is different for each compliance current.*

It can be observed that in each process the set voltage is different. For each process a different device was used and, therefore, the parameters of the memristor can vary.

B. Conduction mechanism

Figure 3 shows that the HRS has not a linear behaviour with the voltage. On the contrary, for the LRS an Ohmic conductions seems to be satisfied. The LRS state has the same behaviour for all the cycles. Using the region of negative voltages from Fig. 3(b) of the LRS, a linear fit has been done [Fig. 7]. As we expected, Ohmic conduction is satisfied with a resistance of 140 Ω, which is a low value in comparison with the resistances in the HRS (order of MΩ).

Assuming that the current through the nanolayers passes through nanofilaments, we can estimate the number of them using the Landauer formula [11]. Conductance is defined as $G=I/V=1/R$. For a quantum channel, the quantum conductance is defined as $G_0=2e^2/h$, where e is the electron charge and h is the Planck constant. The total amount of conductance is the sum of the conductance of each channel, where N is the total number of channels and $G_0 \approx 7.75 \times 10^{-5}\ \Omega^{-1}$. Therefore, $G=(2e^2/h)N$ and we can estimate that N~92.

For the HRS we performed three different possible conduction mechanisms: Schottky (also Richardson-Schottky), Trap assisted tunnelling (TAT) and Poole-Frenkel (P-F). Schottky and TAT are electrode-limited conduction mechanisms, while P-F is a bulk-limited mechanism. In the case of electrode-limited mechanism, the number of injected carriers is mainly governed by the electrode-dielectric potential barrier height instead of by the number of free sites (or defects) in the dielectric layer. On the other hand, the bulk-limited mechanism occurs when at steady state conduction the dielectric cannot evacuate all the carriers supplied by the electrode. TAT did not provide us a good fitting, while P-F adjusted very well to the curve. However, the values for the permittivity extracted with P-F was not suitable. Therefore, Schottky mechanism is the chosen one. In Schottky emission, the action of an external electric field lowers the potential barrier height [Fig. 8].

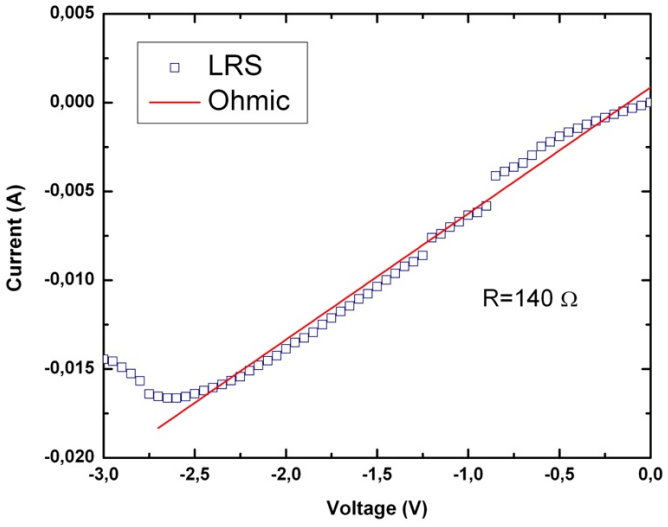

Fig. 7. *Linear fit of the LRS. We report an Ohmic conduction with a resistance of 140 Ω.*

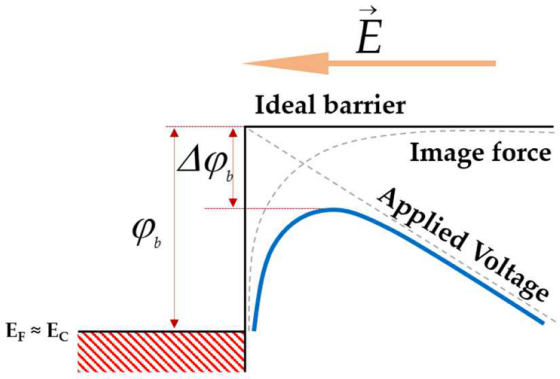

Fig. 8. *Energy band diagram sketch showing the barrier height lowering effect by the application of an external electric field. Extracted from [12].*

This Schottky barrier height lowering is expressed by [12]:

$$\Delta\varphi_b = q\sqrt{\frac{qE}{4\pi\epsilon_0\epsilon_r}} = \beta E \qquad (1)$$

where q is the elementary charge, E the applied electric field (which can be related with the voltage as $E=V/d$) and ϵ_0 and ϵ_r are the absolute and relative permittivity respectively. Therefore, current density is defined as:

$$J_{Schottky} = \frac{4\pi m^*}{h^3} q k_B^2 T^2\, exp\left(\frac{-\varphi_b}{k_B T}\right) exp\left(\frac{\beta\sqrt{E}}{k_B T}\right) \qquad (2)$$

where m^* is the effective mass of the electron and h is the Planck constant. In order to extract these parameters, we have to represent equation (2) in terms of logarithm. Then, a linear fit was used where the slope is $\beta/k_B T$. From the slope we can determine the relative permittivity. Fig. 9(a) and 9(b) shows the fitting using the Schottky barrier mechanism.

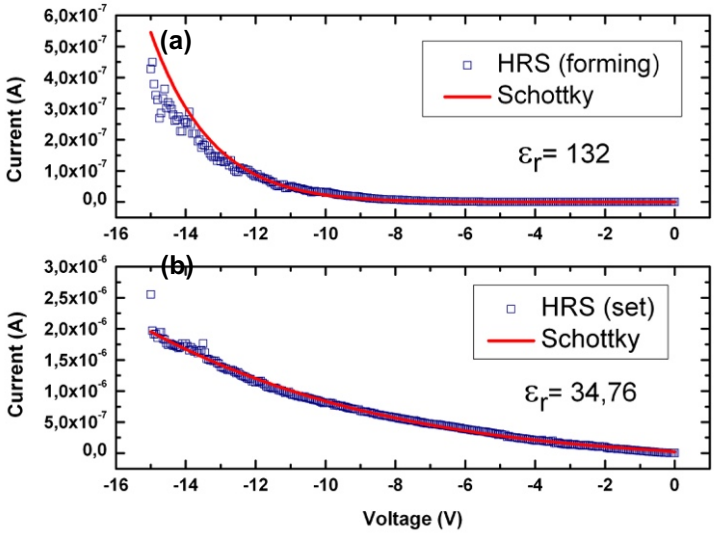

Fig. 9. *Schottky fitting for the HRS state in **(a)** forming and **(b)** set processes. The values extracted from the fitting are very alike, although the value in the set process is more conventional.*

In Fig. 9(a) the fitting was done in the HRS of the forming process (first cycle). For high (negative) voltages the fitting is not so good than for low voltages, but Schottky fit is suitable for this work. However, the parameter extracted is very high in comparison with the literature. For the set process, the Schottky fitting has been carried out with exit [Fig. 9(b)]. In this case, the permittivity is lower but it is still high. In conclusion, we reported a very high values of relative permittivity. The permittivity is defined as the ability of a material to resist an electric field. Therefore, our material is very resistive in comparison with SiO_2, that has a value of 3.9. Another material that is used in memristive devices is titanium dioxide (TiO_2). Titanium dioxide has a permittivity of 63.7 at room temperature [13] which is a value in the order of our material (in the set process).

C. Current-time characteristics

In order to study the set and reset processes we can also study the current-time curve. By applying a constant voltage (pulses) during a certain period of time (60 s), we can see how the current varies. Fig. 10(a) and 10(b) shows current-time under constant voltage for the set process and reset process, respectively. There are fluctuations in current for a constant voltage applied.

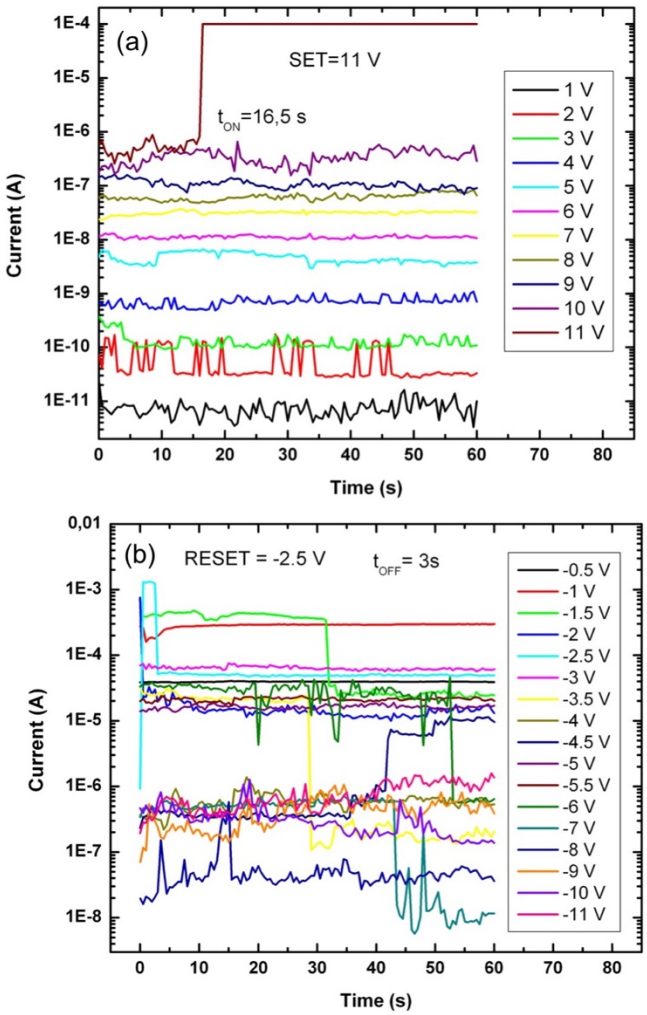

Fig. 10. *Current-time characteristics under a constant voltage from* ***(a)*** *0 to 11 V (set) and* ***(b)*** *-0.5 to -12 V (reset).*

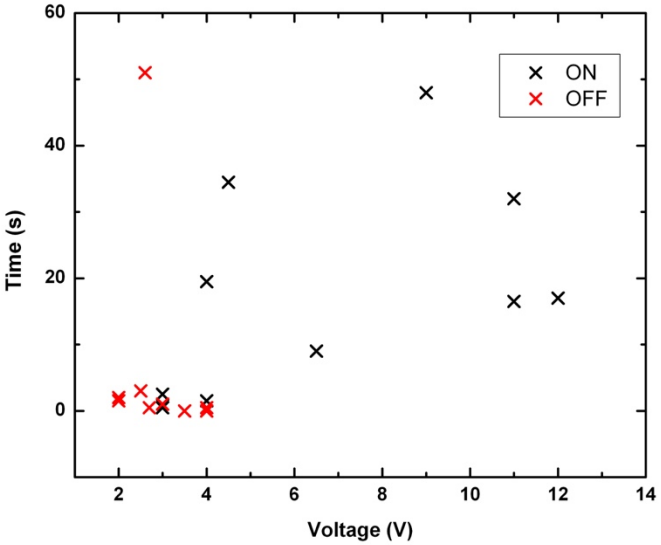

Fig. 11. *Time-voltage characteristics. In black: time needed to pass from HRS to LRS (set). Red: time which the device needs to pass from LRS to HRS (reset), where the voltage is expressed in absolute value. It is clear that for the reset, the time is always lower than the set. For the set process, the dispersion is too high.*

In the set process, these fluctuations are not very high. On the contrary, for the reset process there are more fluctuations in current. With this curve, we can also know the time that the system needs to pass from HRS to LRS and vice versa. In this particular device, the time needed is 16.5 s for the set process (ON) and 3 s for the reset process (OFF). For the set process, if we apply a voltage larger than 11 V, the time needed will be 0 s, because the system is already in the LRS. With this experimental measurement we have been able to see the set and reset processes for our device. The time that the device takes to commute between states is a random parameter. Ideally, for a good logic memory, this time would be as small as possible in order to have a speed device. For the reset time, we achieved low values to pass from ON to OFF. On the contrary, for the forming or set process our values are very high dispersed. Fig. 11 shows the time-voltage curve. As we can observe, the points for the set process (ON) have a huge dispersion error. Therefore, we cannot apply an empirical model to it. For the OFF state, the values are very close to the zero value (with an exception).

D. Comparison of switching characteristics

Our devices are completely electrically characterized and we can extract all the important parameters. In order to stablish if our devices are suitable to work as a memory, we have compared with some other memristive devices present at the literature. Table 1 shows the comparison between our device TbO_x, with SiO_x, NiO_x, TiO_x and HfO_x, which are the most promising materials for memristive applications and have similar switching mechanism. As we can observe, all the memristors have unipolar and bipolar switching mechanism, as a contrast with our devices, which only behaves as a bipolar switching. For the ratio ON/OFF, that is, the ratio between resistances, the value obtained is similar to them. For the operation speed, we only present the value of the reset due to the fact that the set time has a very huge dispersion.

TABLE I

Summary of most important storage media and their respective switching parameters. The operation speed is written as 'set speed; reset speed. For our device only the reset speed is shown.

Storage medium	Switching mode	ON/OFF ratio	Operation speed	Endurance (cycles)
TbO_x	Bipolar	2 x 10^5	1 s	20
SiO_x [14,15,16]	Unipolar, bipolar	10^7	100 ps; 100 ps	10^4
NiO_x [17,18,19]	Unipolar, bipolar	10^6	10 ns; 20 ns	10^6
TiO_x [20,21]	Unipolar, bipolar	10^5	5 ns; 5 ns	2 x 10^6
HfO_x [22,23]	Unipolar, bipolar	10^5	300 ps; 300 ps	10^{10}

Anyway, our value is still very large in comparison with others. Operation speed of the devices are in the range of pico and nano-amperes, where SiOx is the faster. Finally, the number of cycles that the devices can hold (endurance) is a very important parameter. Our devices can only hold 20 cycles at least without suffering damages and all the devices have a very high endurance. For the other devices, is very remarkable the high endurance of HfO_x, which is in concordance with its position as a high-k dielectric.

E. Structural characterization

For the morphological characterization, we employed the second type of samples.

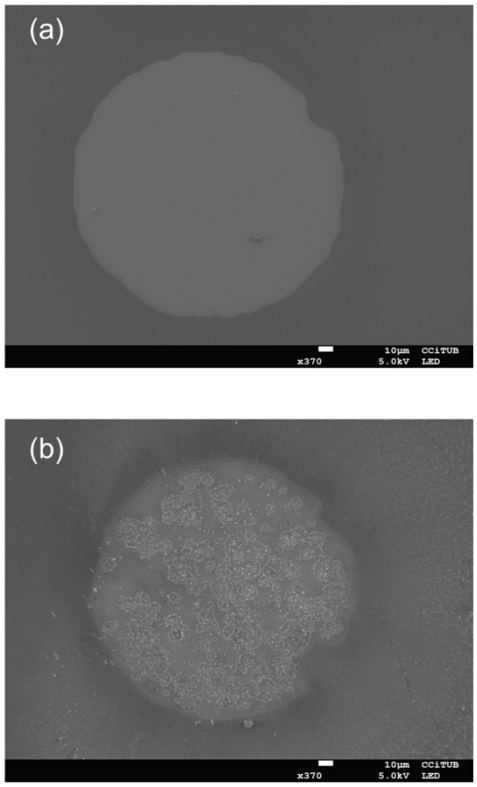

Fig. 12. *SEM images of the memristor device without Tb.* ***(a)*** *Pristine state of the device and* ***(b)*** *device after the set process.*

In this case, the device is the same as the sketch of figure 2 but without the Al/Tb/Al stack. In order to observe if our device follows the VCM, we have increased the presence of oxygen in the nanolayers. These devices are not suitable to perform an electrical characterization. The excess of oxygen causes damages at the device, which was not able to perform any cycle.

In Fig. 12(a) the pristine state of the device is shown. We can observe that the shape of our devices are not perfectly circular. When we are applying voltage to our devices, we will reach the set voltage. Figure 12(b) shows the device when it has been arrived to this point, where a lot of holes appear. These all holes are caused by the excess of oxygen. It is important to mention that terbium is not present in these samples. It seems that the presence of terbium can help to retain the oxygen atoms and allow the device to commute between the two states without permanent damages. The excess of oxygen seems to be a problem due to the fact that exists a disarray of the oxygen atoms in the device. In order to fully characterize the samples, we used the EDS technique to know the elements present in the device. In Fig. 13(a) are showed the points selected to perform EDS and Fig. 13(b) shows their spectrum for all the points. It is important to remember that the electrodes were made by aluminium and the substrate is silicon.

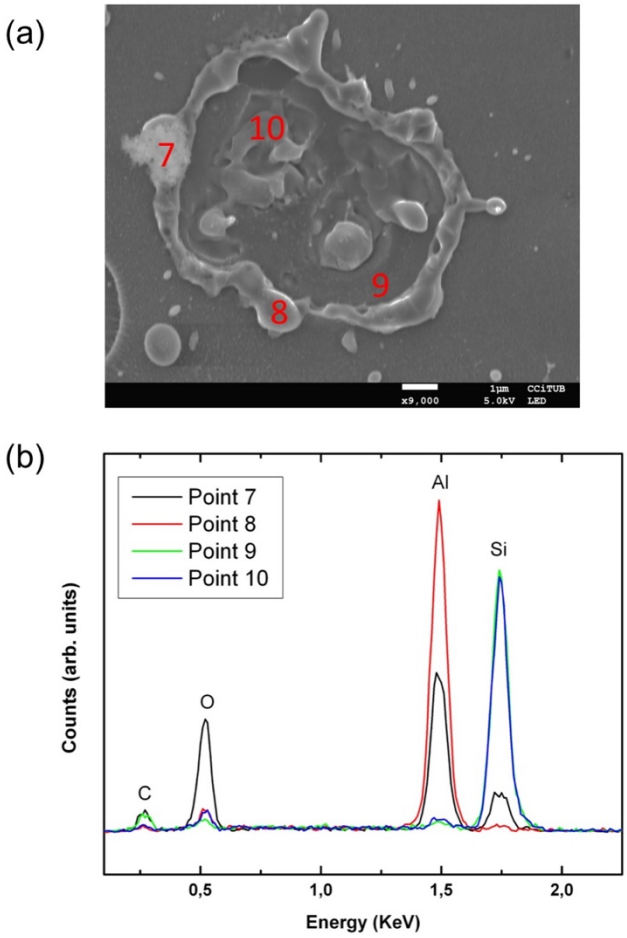

Fig. 13. ***(a)*** *Zoom of one hole.* ***(b)*** *EDS spectrum of the four points marked in* ***(a)****. There are four peaks that correspond to each element.*

This can be related with the presence of silicon at points 9-10, where the hole is so deep that we can observe the substrate. Point 7 is an interesting point due to its appearance and the mixture of elements observed. We can observe oxygen, aluminium and silicon. It is the only point where oxygen is observed. Finally, point 8 shows only the presence of aluminium, due to the fact that is the outline of the hole. The presence of carbon is very low in all the points, due to it is a residual element in our devices.

F. Switching model

Using the structural characterization of our samples, we demonstrate that oxygen is moving through our layers. Therefore, valence change mechanism is the responsible for the memristive behaviour of the devices. Fig. 14 shows a sketch for this process. First of all, the pristine state of the sample is shown [Fig. 14(a)]. After applying a certain voltage to the top electrode, the anions will go to the bottom electrode. A conductive filament (CF) is starting to grow [Fig. 14(b)]. Fig. 14(c) shows the forming process: the system reach enough voltage to form a CF that connects the two electrodes. By applying a negative voltage, the anions will go in the opposite direction and the CF will be disrupted. This is the reset process, shown in figure 14(d). From this point, the system will pass from the step (c) to (d) by changing the polarity of the voltage. This model is only valid for bipolar switching due to the necessity of change the polarity.

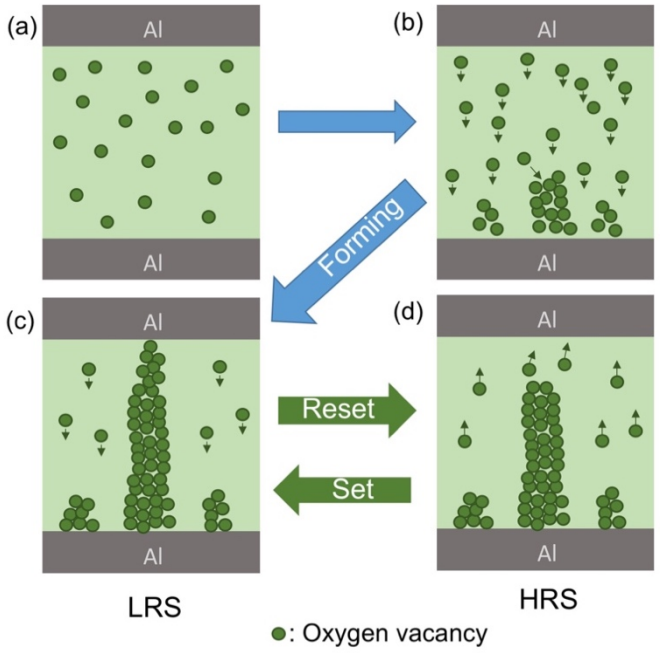

Fig. 14. *Sketch of the VCM. The arrows indicate the migration direction of the anions. We can distinguish four steps:* ***(a)*** *pristine state of the device,* ***(b)*** *a difference of voltage is applied to the electrodes and oxygen anions go to the bottom electrode, where a conduction filament (CF) is starting to grow,* ***(c)*** *CF is formed and the forming process is reached and* ***(d)*** *by applying a negative voltage, the anions start to go at the opposite direction and the CF is disrupted. Readapted from [24].*

IV. CONCLUSION

In summary, we have demonstrated that our Al/Tb/SiO_2 nano-multilayer devices fabricated by electron beam evaporation shown resistive switching mechanism. Forming, set and reset processes are observed and all the characteristics and parameters are extracted. We reported a high difference between the resistance in the HRS and the LRS. The devices can commute between states during at least 20 cycles, with a low dispersion in the set and reset voltages. Set voltages are too high to use this system as a non-volatile memory. We have shown bipolar switching mechanism, due to the necessity to change the polarity of voltage to perform the reset process. We stablish a range of work in terms of the current compliance between 1 to 10^4 μA.

The study of which conduction mechanism is carrying out our resistive switching gives us the conclusion that an Ohmic conduction follows the LRS and Schottky conduction the HRS. We have been able to estimate that there are approximately 92 filaments at the LRS. Schottky conduction give us two different values for the relative permittivity at the HRS for the forming process and the set process, which are high values: 132 and 34.8, respectively.

Current-time characteristics show the fluctuations in time of the current under a constant voltage. These fluctuations are very interesting due to the fact that charge movement are taking place in the device. We have been also able to determine the time speed to commute between two resistance states. Time to pass from LRS to HRS is generally very low. On the contrary, for the time to pass from HRS to LRS, we observe a high dispersion in the values and we have determined that this time has a random behaviour.

Comparing our devices with literature, we have been able to extract some defects and benefits of the samples. The ratio between resistances in ON and OFF state is very similar with other devices. On the contrary, for the endurance and speed operation a long way is still necessary to reach these devices. It is important to mention that our devices are fabricated with electron beam evaporation and the goal is study the memristive behaviour of them. They are not thought to work as a commercial memory.

Structural characterization with SEM images and EDS spectrum help us to stablish the conclusion that oxygen vacancies are moving inside our samples. We have been able to observe with another type of samples which is the role of terbium and the annealing process. Introduce terbium and perform an annealing after the fabrication helps the device to observe the resistive switching mechanism.

Valence change mechanism is the responsible for the resistive switching mechanism in our devices. We report an interpretation of how the mechanism is carrying out and the conduction filament is created and disrupted by changing the polarity of the voltage applied.

ACKNOWLEDGEMENT

Firstly, I would like to express my sincere gratitude to my advisors Dr. Blas Garrido and Oriol Blázquez for their continuous support and guidance. Besides my advisors, I would like to thank Dr. Sergi Hernández for his insightful comments.

I would also like to mention the friends that I met this year during the master course. I hope you the best.

Finally, I would like to thank my family and friends for their support.

REFERENCES

[1] Chua, L. (1971). Memristor-the missing circuit element. *IEEE Transactions on circuit theory*, *18*(5), 507-519.

[2] Strukov, D. B., Snider, G. S., Stewart, D. R., & Williams, R. S. (2008). The missing memristor found. *Nature*, *453*(7191), 80-83.

[3] Mehonic, A., & Kenyon, A. J. (2015). Resistive switching in oxides. In *Defects at Oxide Surfaces* (pp. 401-428). Springer International Publishing.

[4] Mehonic, A., Cueff, S., Wojdak, M., Hudziak, S., Labbé, C., Rizk, R., & Kenyon, A. J. (2012). Electrically tailored resistance switching in silicon oxide. *Nanotechnology*, *23*(45), 455201.

[5] Mehonic, A., Cueff, S., Wojdak, M., Hudziak, S., Jambois, O., Labbé, C., Garrido, B., Rizk, R. & Kenyon, A. J. (2012). Resistive switching in silicon suboxide films. *Journal of Applied Physics*, *111*(7), 074507.

[6] Kim, D. C., Seo, S., Ahn, S. E., Suh, D. S., Lee, M. J., Park, B. H., ... & Lee, J. E. (2006). Electrical observations of filamentary conductions for the resistive memory switching in NiO films. *Applied physics letters*, *88*(20), 202102.

[7] Pickett, M. D., Strukov, D. B., Borghetti, J. L., Yang, J. J., Snider, G. S., Stewart, D. R., & Williams, R. S. (2009). Switching dynamics in titanium dioxide memristive devices. *Journal of Applied Physics*, *106*(7), 074508.

[8] Kumar, S., Wang, Z., Huang, X., Kumari, N., Davila, N., Strachan, J. P., ... & Williams, R. S. (2017). Oxygen migration during resistance switching and failure of hafnium oxide memristors. *Applied Physics Letters*, *110*(10), 103503.

[9] Mehonic, A., & Kenyon, A. J. (2016). Emulating the electrical activity of the neuron using a silicon oxide RRAM cell. *Frontiers in neuroscience*, *10*.

[10] Gaba, S., Knag, P., Zhang, Z., & Lu, W. (2014, June). Memristive devices for stochastic computing. In *Circuits and Systems (ISCAS), 2014 IEEE International Symposium on* (pp. 2592-2595). IEEE.

[11] Landauer, R. (1957). Spatial variation of currents and fields due to localized scatters in metallic conduction. *IBM Journal of Research and Development*, *1*(3), 223-231.

[12] Ramírez, J.M. (2015). *Rare Earth-Doped Silicon-Based Light Emitting Devices: Towards new Integrated Photonic Building Blocks* (Doctoral thesis). Universitat de Barcelona, Barcelona, Spain.

[13] Wypych, A., Bobowska, I., Tracz, M., Opasinska, A., Kadlubowski, S., Krzywania-Kaliszewska, A., ... & Wojciechowski, P. (2014). Dielectric properties and characterisation of titanium dioxide obtained by different chemistry methods. *Journal of Nanomaterials*, *2014*.

[14] Choi, B. J., Torrezan, A. C., Norris, K. J., Miao, F., Strachan, J. P., Zhang, M. X., ... & Williams, R. S. (2013). Electrical performance and scalability of Pt dispersed SiO_2 nanometallic resistance switch. *Nano letters*, *13*(7), 3213-3217.

[15] Li, Y., Sinitskii, A., & Tour, J. M. (2008). Electronic two-terminal bistable graphitic memories. *Nature Materials*, *7*(12), 966-971.

[16] Song, S. J., Seok, J. Y., Yoon, J. H., Kim, K. M., Kim, G. H., Lee, M. H., & Hwang, C. S. (2013). Real-time identification of the evolution of conducting nano-filaments in TiO_2 thin film ReRAM. *Scientific reports*, *3*.

[17] Baek, I. G., Lee, M. S., Seo, S., Lee, M. J., Seo, D. H., Suh, D. S., ... & Chung, U. I. (2004, December). Highly scalable nonvolatile resistive memory using simple binary oxide driven by asymmetric unipolar voltage pulses. In *Electron Devices Meeting, 2004. IEDM Technical Digest. IEEE International* (pp. 587-590). IEEE.

[18] Yoshida, C., Kinoshita, K., Yamasaki, T., & Sugiyama, Y. (2008). Direct observation of oxygen movement during resistance switching in NiO/Pt film. *Applied Physics Letters*, *93*(4), 042106.

[19] Lee, M. J., Park, Y., Suh, D. S., Lee, E. H., Seo, S., Kim, D. C., ... & Seo, D. H. (2007). Two series oxide resistors applicable to high speed and high density nonvolatile memory. *Advanced Materials*, *19*(22), 3919-3923.

[20] Yoshida, C., Tsunoda, K., Noshiro, H., & Sugiyama, Y. (2007). High speed resistive switching in $Pt/TiO_2/Ti$ N film for nonvolatile memory application. *Applied Physics Letters*, *91*(22), 223510.

[21] Song, S. J., Seok, J. Y., Yoon, J. H., Kim, K. M., Kim, G. H., Lee, M. H., & Hwang, C. S. (2013). Real-time identification of the evolution of conducting nano-filaments in TiO_2 thin film ReRAM. *Scientific reports*, *3*.

[22] Miranda, E. A., Walczyk, C., Wenger, C., & Schroeder, T. (2010). Model for the Resistive Switching Effect in HfO_2 MIM Structures Based on the Transmission Properties of Narrow Constrictions. *IEEE Electron Device Letters*, *31*(6), 609-611.

[23] Chen, Y. Y., Goux, L., Clima, S., Govoreanu, B., Degraeve, R., Kar, G. S., ... & Jurczak, M. (2013). Endurance/Retention Trade-off on HfO_2 Cap 1T1R Bipolar RRAM. *IEEE Transactions on electron devices*, *60*(3), 1114-1121.

[24] Pan, F., Gao, S., Chen, C., Song, C., & Zeng, F. (2014). Recent progress in resistive random access memories: materials, switching mechanisms, and performance. *Materials Science and Engineering: R: Reports*, *83*, 1-59.